Visualizing hydraulic zones of a vertical circulation well in presence of ambient flow

Qiang Xia[a,b], Qiang Zhang[a,*], Mo Xu[a], Yi-ge Tang[a], Hao-wen Teng[a]

[a]*State Key Laboratory of Geohazard Prevention and Geoenvironment Protection, Chengdu University of Technology, 1#, Dongsanlu, Erxianqiao, Chengdu 610059, Sichuan, P.R.China, Tel. +86 182 0289 2357; emails: zhangq@cdut.edu.cn (Q. Zhang), xiaqiang2012@cdut.cn (Q. Xia), Tel. +86 138 0803 5375; emails: xm@cdut.edu.cn (M. Xu), 1791686899@qq.com (Y.G. Tang), 340597108@qq.com (H.W. Teng)*
[b]*Department of Earth and Atmospheric Sciences, University of Nebraska-Lincoln, 1400 R Street, Lincoln, Nebraska, 68588, USA*

ABSTRACT

Although vertical circulation well (VCW) has been widely applied for aquifer remediation and hydrogeological parameter estimation for three decades, few studies have focused on the hydraulic zone visualization, and the spatial scale of hydraulic zones as functions of VCW parameters. This study provided a numerical method to visualize 3D steady-state flow field induced by VCW in a confined aquifer in presence of an ambient flow. Mathematical model for velocity field is established based on the superposition principle, and the fourth-order Runge-Kutta method is adopted to perform particle tracking. Visualization results illustrate that 3D flow regime can be divided into Recirculation, Capture, and Discharge zones. An integrated dimensionless parameter Q_D is introduced to account for the relative strength of VCW flow against ambient flow. Comparison is performed through simulations by different Q_D–d_D combinations, where d_D is the dimensionless distance between injection and extraction screens. Results demonstrate that: (1) a Q_D–d_D breakthrough line can be established to mark the occurrence of circulatory flow; (2) the effect of Q_D on the size of recirculation zone is significant when Q_D is smaller than 3.5, while d_D becomes more influential if Q_D is larger; (3) the extent of capture and discharge zone enlarges as Q_D and/or d_D increases.

Keywords: Vertical circulation well; Ambient flow; Particle tracking; Recirculation zone; Capture zone

1. Introduction

A vertical circulation well (VCW) is a vertical well or borehole consisting of two screened sections separated by an impermeable casing with a small pump circulating water between the upper and lower chamber [1]. The groundwater flow induced by a VCW is also called "a dipole flow", and characterized by: (1) vertical circulatory flow, which is distinct from the conventional injection-extraction double well system, generating a horizontal circulation; (2) axisymmetric pattern in the absence of ambient flow; (3) the relatively quickly established steady state; (4) no net withdrawal of water from the aquifer, and so on. It is worth noting that another term Groundwater

Circulation Wells (GCW or GZB in German) is also widely used in literature [2–4], however, some of them only concerned with horizontal circulation and the vertical circulation didn't occur mostly due to the presence of an internal aquitard.

Practical applications of VCW in groundwater industry include aquifer remediation, hydrogeological parameter determination, dewatering [5] and more recently aquifer storage and recovery management regarding the use of dipole flow to make a fresh water lens in a static saline groundwater [6]. As a recirculation system, VCWs have become an effective technology for in situ aquifer remediation, when coupled with a number of chemical and biological approaches [4]. Knox et al. [7] assessed the ability of the VCW system

* Corresponding author.

for controlling chemical extractants that were added to the subsurface. Cirpka and Kitanidis [8] presented a travel-time based approach for modeling bioreactive transport in a flow field caused by a series of VCWs. Zhao et al. [9] investigated the efficacy of biofilms formed in a VCW for in situ bioremediation of aniline-contaminated groundwater.

In addition, VCW are applied in aquifer characterization. It was first introduced in the petroleum industry to determine the vertical permeability in petroleum reservoirs [10]. Since 1994, numerous dipole flow test (DFT) were performed at various sites around the world [11–14]. In light of analytical solutions developed by [1,15], it became possible to apply VCW for aquifer parameter estimation. Kabala [15] proposed the Newton-Raphson iterative algorithm for estimation of both horizontal and vertical hydraulic conductivity, and a specific storage coefficient for transient case. Zlotnik and Zurbuchen [13] designed a dipole probe (DP) to measure vertical variations of hydraulic conductivity, and the DP has been successfully tested in a highly conductive sand and gravel aquifer. Apart from analytical solution, Hvilshøj et al. [14] proposed an inverse numerical model for parameter identification. By releasing tracer into the injection screen, and recording the concentration breakthrough curve in the extraction, Sutton et al. [16] developed dipole flow test with a tracer (DFTT), and adopted a semi-analytical simulation to determine the longitudinal dispersivity. Nevertheless, Chen et al. [17] suggested that longitudinal dispersivity cannot be solely determined by analysis of the breakthrough curve in DFTT, because the test is simultaneously affected by both the longitudinal and transverse dispersions.

In order to use VCW system effectively and efficiently, it is important to know the nature and extent of the induced groundwater flow field. Herrling et al. [18] first employed numerical simulation to present a view of three water bodies around a VCW, namely the captured, circulating and flowing downstream water. In the absence of ambient flow, Zlotnik and Ledder [1] suggested the region of influence of a VCW may be taken to be the region within the stream surface containing 90% of the flow. As a result, the region of influence extends to approximately five distances between chamber centers in the radial direction and two distances in the vertical. Philip and Walter [19] revealed that increasing the separation distance between injection and extraction intervals increased the width of the capture zone. Huang and Goltz [20] developed a three-dimensional analytical solution to map the spatial extent of capture zone resulting from operation of a tandem circulation wells. Based on comprehensive data set and numerical model, Johnson and Simon [21] defined the time-dependent recirculation zone and capture zone for a real VCW site. Chen et al. [22] developed a mathematical model for describing reagent transport in a VCW flow field, which is the first attempt to delineate the spatial distribution of the solute. Although the flow pattern has been extensively studied, there is still a lack of understanding of the spatial arrangements of various hydraulic zones.

Therefore, the objectives of this study are: (1) to provide tools for visualization of flow field induced by a single VCW, (2) to define distinct hydraulic zones, (3) to explore the unique property of these zones, and (4) to investigate the geometry of hydraulic zones as a function of various VCW parameters.

2. Problem description

In this study, we consider the flow field induced by a VCW in a confined aquifer. The following assumptions are used for the development of the mathematical model. (1) the aquifer thickness b is constant and the aquifer is boundless sidewise; (2) the aquifer is homogeneous and isotropic; (3) a uniform and steady-state ambient flow occurs in the aquifer; (4) the flow field is steady; (5) the density effect is neglected; (6) the well has no skin zone.

The concerned VCW consists of a single well with two screened sections, an upper injection screen and a lower extraction screen as shown in Fig. 1, each screen has a length $2L$. We define a 3D Cartesian coordinate system, where $x = y = 0$ is VCW located, the bottom of the aquifer at $z = 0$, with the positive direction pointing up, and the top of the aquifer located at $z = b$. The distance between two screen centers is d. z coordinates for the two centers are denoted as z_u and z_l respectively. The center of the aquifer is z_c as $z_c = b/2$. Each screen section is idealized as a uniform line source or sink with total flow rate Q, negative sign for water extraction and positive sign for water injection. The radius of VCW is r_w.

We assume the ambient flow is parallel to the x-axis and in the positive direction with a hydraulic gradient J. Both horizontal and vertical hydraulic conductivities of the aquifer are K.

The steady-state vertical circulation flow field induced by the VCW in a homogeneous and isotropic aquifer can be modeled by using the method provided by Philip and Walter [19], which begins with the hydraulic head solution for a point sink in an infinite aquifer. The point sink is then integrated to derive the solution for a line sink. Linear superposition is applied to obtain the hydraulic head resulting from multiple line sinks and sources in a homogeneous confined aquifer. We also take the extraction screen to be a line sink, and injection as a line source. Consider a line sink of length $2L$ centered at $x = 0$, $y = 0$, $z = z_0$ ($L \leq z_0 \leq b-L$) in a Cartesian coordinates, the solution for head distribution is:

$$h(x,y,z) = \frac{-Q}{8\pi KL} \times \ln\left[\frac{z - z_0 + L + \sqrt{x^2 + y^2 + (z - z_0 + L)^2}}{z - z_0 - L + \sqrt{x^2 + y^2 + (z - z_0 - L)^2}}\right] \tag{1}$$
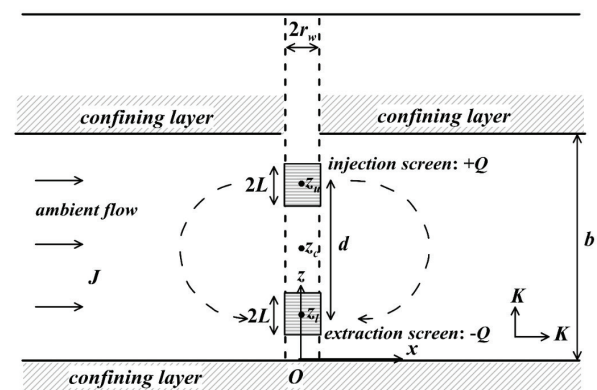
Fig. 1. 2D schematic diagram of a vertical circulation well (modified after Chen et al. [17]).

This equation describes the head change at any location in an infinite aquifer caused by a line sink. It is then differentiated to obtain the hydraulic head gradient and three-dimensional velocity field.

$$v_x = \frac{-K}{n_e}\frac{\partial h}{\partial x}; \quad v_y = \frac{-K}{n_e}\frac{\partial h}{\partial y}; \quad v_z = \frac{-K}{n_e}\frac{\partial h}{\partial z} \tag{2}$$

$$\frac{\partial h}{\partial x} = \frac{-Qx}{8\pi KL}$$
$$\times \left[\frac{1}{A\cdot(z - z_0 + L + A)} - \frac{1}{B\cdot(z - z_0 - L + B)} \right] \tag{3}$$

$$\frac{\partial h}{\partial y} = \frac{-Qy}{8\pi KL}$$
$$\left[\frac{1}{A\cdot(z - z_0 + L + A)} - \frac{1}{B\cdot(z - z_0 - L + B)} \right] \tag{4}$$

$$\frac{\partial h}{\partial z} = \frac{-Q}{8\pi KL}\left[\frac{1}{A} - \frac{1}{B} \right] \tag{5}$$

$$A = \sqrt{x^2 + y^2 + (z - z_0 + L)^2};$$
$$B = \sqrt{x^2 + y^2 + (z - z_0 - L)^2} \tag{6}$$

where v_x, v_y, v_z is x, y, z component of velocity respectively, n_e is effective porosity of aquifer.

By employing the principle of linear superposition, a line sink centered at one location may be mated with a line source centered above or below it to simulate the effect of a vertical circulation well in an infinite aquifer. Similarly, for a confined aquifer the presence of upper and lower confining beds may be accounted for by adding image sources and sink for each real one [23]. Then the overall velocity field can be determined by summing all the individual velocity contribution from both real and virtual line sources and sinks to obtain the net velocities. In addition, the effect of the ambient flow gradient may be included by simply adding the solutions of the x component [19].

$$V_x = \sum_{n=2}^{N} v_x + \frac{JK}{n_e}; \quad V_y = \sum_{n=2}^{N} v_y; \quad V_z = \sum_{n=2}^{N} v_z \tag{7}$$

Since two boundaries are involved in this paper, an infinite number of image line sources and sinks are required theoretically, which means the number N in Eq. (7) should be infinite. In practice, however, N can be a finite number as long as we set an acceptable tolerance ε for the change of velocity. We found that setting the tolerance ε equal to 10^{-7} worked well for most cases. Because all the line sources and sinks are centered at $x = 0$, $y = 0$ but different z_0, so when we calculate the velocity for a given point (x, y, z) by using Eq. (7), merely the z_0 and Q need to be changed for the variety of line sources or sinks.

3. Methods of particle tracking

It is hard to obtain closed form expressions for streamlines in our case, thus we resort to numerical methods. Runge-Kutta method [19,24–26] can be applied to trace particle paths in three dimensions based on the velocity vector Eq. (7). We adopted the fourth-order Runge-Kutta algorithm to advance a particle from the initial position (x_n, y_n, z_n) over a time interval Δt, the position of the particle at the beginning of the next step $(x_{n+1}, y_{n+1}, z_{n+1})$ is calculated as:

$$x_{n+1} = x_n + \frac{(k_1 + 2k_2 + 2k_3 + k_4)}{6} \tag{8a}$$

$$y_{n+1} = y_n + \frac{(l_1 + 2l_2 + 2l_3 + l_4)}{6} \tag{8b}$$

$$z_{n+1} = z_n + \frac{(m_1 + 2m_2 + 2m_3 + m_4)}{6} \tag{8c}$$

Where:

$$k_1 = \Delta t V_x(x_n, y_n, z_n); \quad l_1 = \Delta t V_y(x_n, y_n, z_n);$$
$$m_1 = \Delta t V_z(x_n, y_n, z_n) \tag{9}$$

$$k_2 = \Delta t V_x\left(x_n + \frac{k_1}{2}, y_n + \frac{l_1}{2}, z_n + \frac{m_1}{2}\right) \tag{10a}$$

$$l_2 = \Delta t V_y\left(x_n + \frac{k_1}{2}, y_n + \frac{l_1}{2}, z_n + \frac{m_1}{2}\right) \tag{10b}$$

$$m_2 = \Delta t V_z\left(x_n + \frac{k_1}{2}, y_n + \frac{l_1}{2}, z_n + \frac{m_1}{2}\right) \tag{10c}$$

$$k_3 = \Delta t V_x\left(x_n + \frac{k_2}{2}, y_n + \frac{l_2}{2}, z_n + \frac{m_2}{2}\right) \tag{11a}$$

$$l_3 = \Delta t V_y\left(x_n + \frac{k_2}{2}, y_n + \frac{l_2}{2}, z_n + \frac{m_2}{2}\right) \tag{11b}$$

$$m_3 = \Delta t V_z\left(x_n + \frac{k_2}{2}, y_n + \frac{l_2}{2}, z_n + \frac{m_2}{2}\right) \tag{11c}$$

$$k_4 = \Delta t V_x\left(x_n + k_3, y_n + l_3, z_n + m_3\right) \tag{12a}$$

$$l_4 = \Delta t V_y\left(x_n + k_3, y_n + l_3, z_n + m_3\right) \tag{12b}$$

$$m_4 = \Delta t V_z\left(x_n + k_3, y_n + l_3, z_n + m_3\right) \tag{12c}$$

Once a particle is initially set up somewhere, the series of calculation is repeated to move the particle step by step until a termination criterion is met, therefore a streamline could be delineated based on all the position records for every step. A particle initially starts from injection screen, if it arrives at the extraction screen, the particle is assumed to have been recirculated, otherwise if the particle flows downstream along with the ambient flow, it is assumed to have been discharged from injection screen. A particle released at some place upstream from VCW, flows as driven by ambient flow, if it eventually reaches the extraction screen, the particle is regarded to be captured, or it would bypass the VCW. So generally four types of streamlines may be identified surrounding a VCW, namely the Recirculated, Captured, Discharged, and Bypassed as shown in Fig. 2.

Assembling plenty of streamlines of the same type forms a unique hydraulic zone, however it requires massive calculation. In practice, the 3D spatial surface that partitions different hydraulic zones is of more interest. Thus a search process is required to find those streamlines that compose a partition surface. If we want to represent the recirculation surface or capture surface by M streamlines, the particle tracking procedure should be solved M times, and each time with a different initial point. For example, a vertical cross section where particle tracking starts is divided into M levels in the z direction as illustrated in Fig. 2(a), then the search procedure is applied for each level to locate the critical point where the outermost captured streamline is. The thought of dichotomy is chosen for the search procedure as shown in Fig. 2(b). Provided that point 1 is captured and point 2 is bypassed in the current Nth search step, thus the middle point 3 is either captured or bypassed. If it is bypassed, then the search for next $N+1$ step should be taken between point 1 and 3, to determine whether their middle point 4 is captured or bypassed. Or if point 3 is captured, the search is constrained between point 2 and 3. After sufficient iteration, that critical point could be approached with satisfactory accuracy.

Similarly the discretization and search procedure are applied for the determination of recirculation surface. The perimeter of injection screen is split up to M pieces with uniform degree interval, see Fig. 2(c), for every piece the search procedure could find the critical z coordinate where the

recirculated and discharged streamlines are delimited. So, particles starting on injection screen all have the same distance to the center of VCW, which is the radius of well r_w. In this way r_w is involved in the particle tracking, even though it is irrelevant with the governing equation that controls the flow field [see Eqs. (1)–(7)].

It is worth noting that particles can also be tracked backwards in the "upstream" direction or from sink to source. It could be achieved by simply assigning the time interval Δt to be negative in Eqs. (9)–(12). Discharge surface is actually determined by the backwards particle tracking technique, all the tracking processes start on a cross section downstream from VCW.

There exists four possible sources to cause the numerical errors of the method constructing a 3D surface developed in this work: (1) the velocity change tolerance ε accounted for the boundary condition; (2) the time increment Δt in Runge-Kutta algorithm [see Eqs. (9)–(12)]; (3) the resolution of a surface, more specifically, the amount of streamlines M to comprise a surface, and (4) the number of iteration N_{iter} for the critical point search procedure. Ideally the smaller ε and Δt, plus larger M and N_{iter} leads to more precise surface, however it requires tremendous calculation and a quite time-consuming process. As mentioned before, it was found that $\varepsilon = 10^{-7}$ could be adopted to establish a reliable result. Through experience, $M = 100$ and $N_{iter} = 10$ provide sufficient and precise data to define a surface. We performed an adaptive scheme to account for the time increment, that is small Δt for high velocity and large Δt for low velocity, to make sure the maximum displacement in any direction for each step is less than a tolerance, which was taken as the radius of VCW r_w.

The theoretical approach described above was implemented by using Matlab R2016.

4. Hydraulic zones visualization

Both 2D and 3D visualization for hydraulic zones are provided in this section. All calculations have accounted for the following parameters as shown in Table 1. Except for the flow rate, all other parameters were kept as constant in different cases.

Fig. 2. (a) 3D schematic diagram of particle tracking in a VCW flow field with an ambient flow, streamlines can be classified into four types: Recirculated (red), Captured (blue), Discharged (green), and Bypassed (grey), arrows indicate the flow direction; (*b*) the bisection search procedure for critical point; (*c*) the layout of starting point on injection screen.

Table 1
Parameters used for hydraulic zones visualization

Parameter	Value
Aquifer thickness (b)	30 m
Half-length of screens (L)	3 m
Vertical coordinate of center of upper screen (z_u)	22 m
Vertical coordinate of center of lower screen (z_l)	8 m
Distance between centers of screens (d)	14 m
Hydraulic conductivity (K)	10 m/d
Ambient flow hydraulic gradient (J)	0.001
Effective porosity of aquifer (n_e)	0.2
VCW flow rate ($Q_I = -Q_E$)	$1 \times 10^{-1} - 1 \times 10^6$ m³/d
Well radius (r_w)	0.1 m

4.1. Flow field on a typical cross section

2D flow field surrounding a single VCW in a confined aquifer is presented on a particular longitudinal cross section in the direction of ambient flow. This cross section is the X–Z plane with $y = 0$ in this paper, the flow situation can only be calculated and plotted in such a 2D view on this cross section, otherwise the complex 3D flow field has to be considered [18].

Fig. 3 exhibits the 2D flow fields for eight cases with varying Q. The red lines stand for the recirculated streamlines, which represent water circulated from the injection screen to the extraction. The black bold line is the most outer recirculated streamline, which delineates the outline of recirculation zone on this X–0–Z plane. The blue lines are for captured streamlines. The green discharged streamlines are plotted by applying backwards particle tracking technique, that the particles tracking is started from a certain transverse cross section downstream VCW. Grey lines stand for the ambient flow bypassing VCW that haven't been captured.

Fig. 3 illustrates the cross-sectional flow field is symmetric with respect to the center of VCW, namely the point of XYZ coordinate $(0, 0, z_c)$. Thus we might be able to infer that the 3D flow regime should be axisymmetric about the central line. This will be discussed in the next section.

Fig. 3 indicates three thresholds for Q are of interest. First, the recirculation zones are similar in plot (a) and (b). Thus, we speculated that there might be a threshold, given a certain tolerance, any larger Q will no longer change the size of recirculation zone. Second, comparison of plot (e) and (f) indicates that a threshold exists, for which the recirculation zone starts to reach the confining layer of the aquifer. Third, it is quite apparent that a threshold between the value of Q for plot (f) and (g), which could be referred to as a breakthrough that circulation flow occurs. These thresholds will be further investigated in the following section.

Knowledge of the stagnation point can also be obtained from above cross-sectional flow field analysis [18], however it is beyond the scope of this paper.

4.2. 3D hydraulic zones

Fig. 4 presents a 3D view of three zones in the vicinity of a VCW in presence of an ambient flow. Specifically, the Recirculation Zone (or Circulation Cell) in the middle,
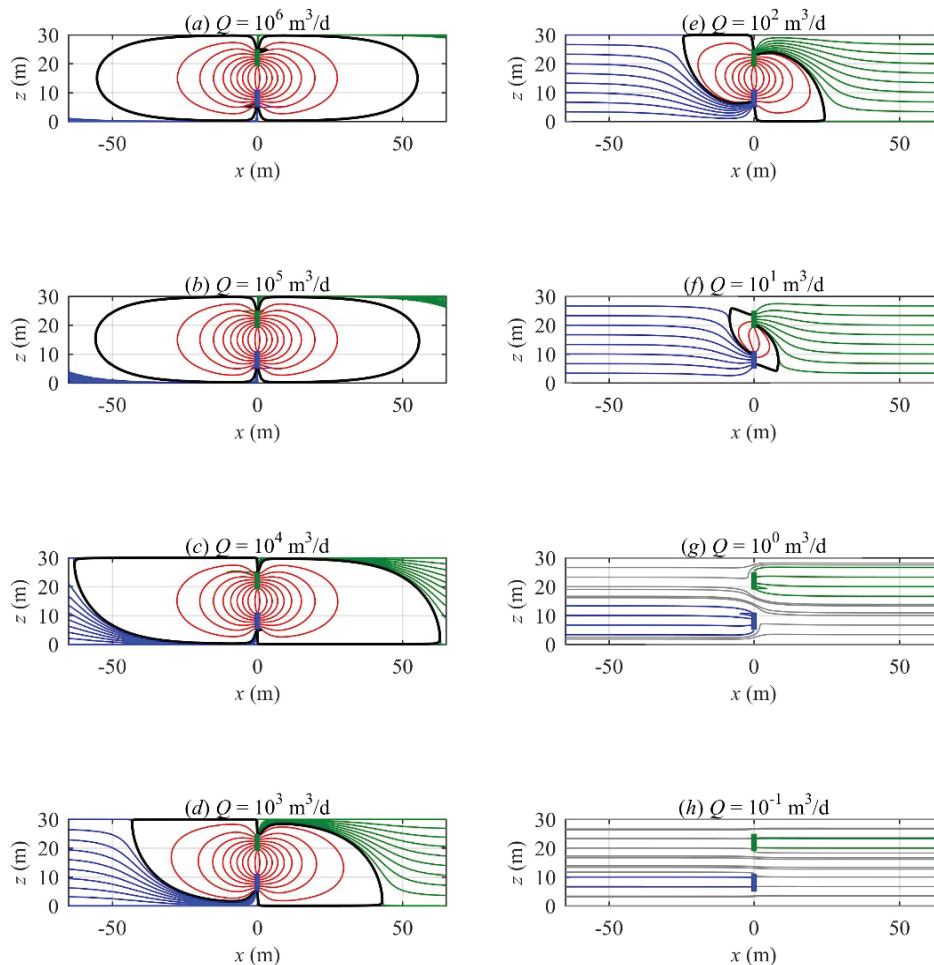
Fig. 3. Comparison of 2D flow field for eight different Q values but constant J. From (a) to (h), Q ranges from 10^6 to 10^{-1} m³ d⁻¹, J is 0.001 for all. Ambient flow is from left side. The green and blue filled areas in the middle of each plot represent the injection and extraction screens.
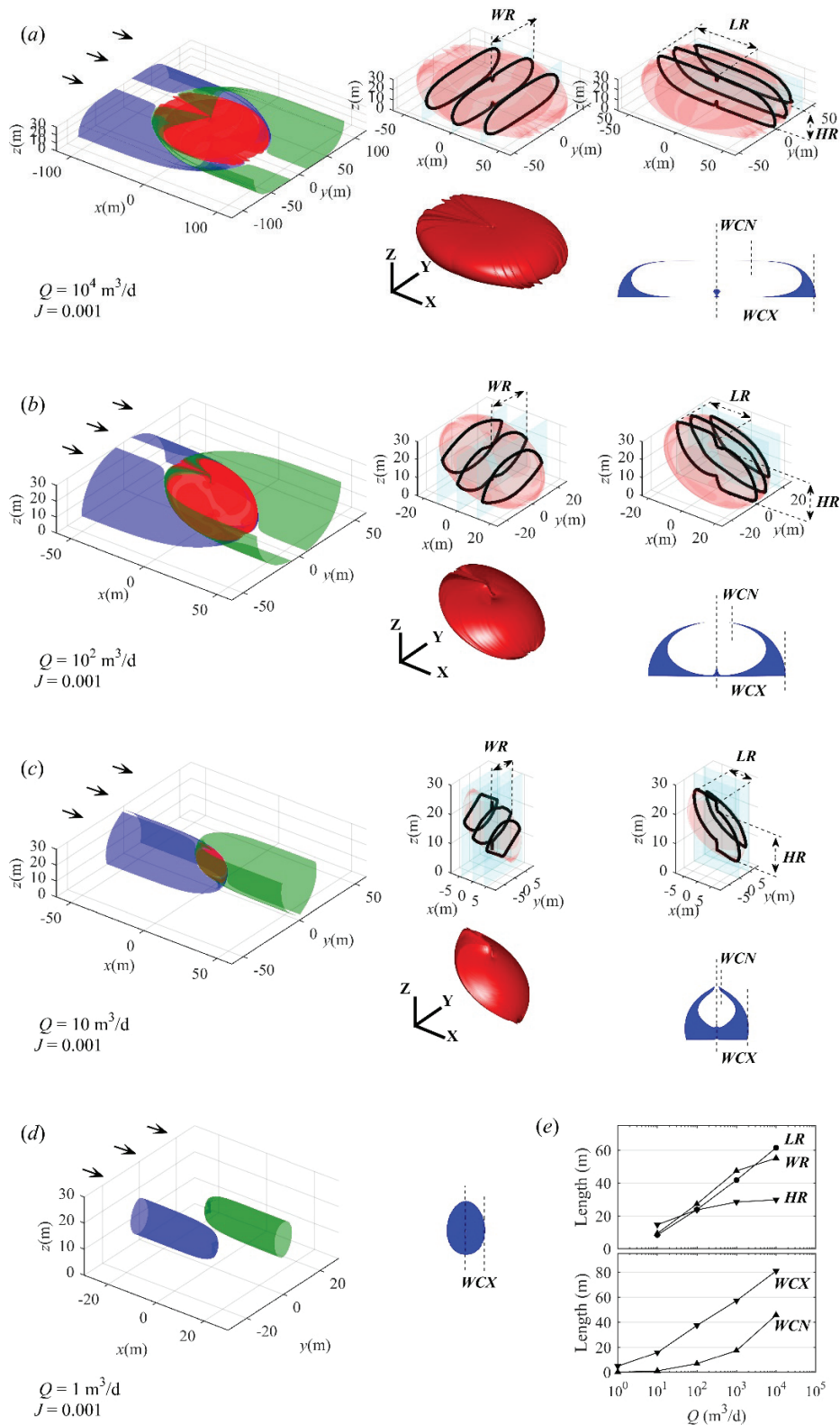
Fig. 4. Visualization of hydraulic zones for four cases: (a) $Q = 10^4$ m^3 d^{-1}, (b) $Q = 10^2$ m^3 d^{-1}, (c) $Q = 10$ m^3 d^{-1}, (d) $Q = 1$ m^3 d^{-1}, respectively, J is 0.001 for all. Plot (e) presents the curves for geometric variables with varying Q. For plot (a), (b), and (c), each plot displays: (1) Visualization of Recirculation, Capture, Discharge zones painted as red, blue, green 3D surfaces respectively, arrows indicate the direction of ambient flow; (2) Transverse and longitudinal cross sections of recirculation zone, notation for geometric variables. (3) Stereogram of recirculation zone; (4) the ultimate cross section of capture zone. Plot (d) only has (1) and (4).

the upstream Capture Zone, and the downstream Discharge Zone are included. Parameters involved are the same as aforementioned in Table 1. Fig. 4 also provides several transverse and longitudinal cross sections of recirculation zone, and a typical cross section for capture zone.

Recirculation zone is located in the middle, surrounded by capture and discharge zones, it looks like a skewed ellipsoid with two poles indented inwards. The water body within this zone outflows from the injection screen, then flows into the extraction screen, to complete a circulation. It consists of cleaned groundwater and circulation flow around the VCW. It is obvious that the shape and extent of recirculation zone is highly sensitive to the value of Q. Given a constant hydraulic gradient of ambient flow J, when Q is decreasing, the recirculation zone will shrink, and finally disappear, see Fig. 4(d). Therefore there should be a critical Q value, for which the recirculation zone starts to shape up. This phenomenon has been verified by the previous 2D cross section results as well.

Parts of ambient flow upstream from the VCW can be captured by the extraction screen, and is delimited by the 3D capture surface. This surface is an imaginary 3D surface that divides the fluid particles moving to the extraction screen from the rest of the ambient flow that bypasses the VCW, which is also called a dividing stream surface [24]. When the VCW flow rate is relatively weaker, ambient flow is more influential, the capture zone cannot reach neither the top of the aquifer nor the bottom, as shown in Fig. 4(c). Theoretically, as long as the ambient flow exists, no matter how strong the VCW flow is, a portion of water outflows from the injection screen cannot flow back into the extraction, and will eventually flow away from VCW due to the effect of ambient flow. Similar to the capture zone, all such water body can be delimited by a 3D surface to form a discharge zone.

Given the direction of the ambient flow is along the axis +X in this paper, it is obvious that the layout of all three hydraulic zones is symmetric with the X–(y = 0)Z plane. In addition, upstream capture zone and the downstream discharge zone are symmetric with respect to the central line, the line of intersection by Y–(x = 0)–Z plane and X–(z = z_c)–Y plane, and this implies the amount of flow captured by extraction screen is identical to that discharged from injection. Moreover, the upstream part of recirculation zone is axisymmetric with its downstream part, as demonstrated by the transverse cross sections of recirculation zone as shown in Fig. 4. Therefore, we can conclude that the entire flow regime is symmetric with respect to the central line of VCW, this axis-symmetry is corresponding to the central point symmetry regarding to 2D flow field in previous section. The characteristic of symmetry is caused by the symmetrical installation of injection and extraction screens, and has nothing to do with the strength of VCW flow Q.

Plots of the transverse and longitudinal cross section in Fig. 4 introduces the notations for the geometry of recirculation zone, denoted as LR, WR, and HR, which represent the maximum length (along axis X), width (axis Y), and height (axis Z) respectively, for half of the recirculation zone. For capture zone, the width is of most interest especially when making a decision for hydraulic design provided a known contamination plume. The width should be measured on cross sections normal to the direction of ambient flow. More importantly, it should be taken at a sufficient distance away

from VCW, to guarantee the extent of any further cross sections did not change. We define two geometric variables to describe the ultimate cross section, WCX and WCN measure the maximum and minimum width for half of cross section respectively. As might expected, if capture zone occupies the entire aquifer, WCX is also the bottom width of capture zone because the extraction screen is set up lower than injection, accordingly WCN is the top width of capture zone.

Plot (e) presents the curves for five geometric variables vs. VCW flow rate Q, given constant ambient flow J. As Q increases, all the five variables increase, thus both recirculation and capture zone extend with increasing Q. Specifically, we further demonstrate how the geometry of VCW hydraulic zones is affected by other parameters in the following sections.

5. Results and discussion

The flow pattern induced by VCW depends on a variety of engineering and design parameters such as the pumping rate Q, half-length of screen sections L, distance between screens d, and well diameter $2r_w$. Chen et al. [17] assessed the influence of operational parameters on breakthrough curves in DFTT including the lengths of the screen, the screen distance. Jin et al. [5] investigated how the separation length of the screen intervals influences the drawdown in a unconfined aquifer. Nevertheless, few concerns with the effect of VCW parameters on the shape of hydraulic zone. Therefore, it is appropriate to quantitatively assess the impact of parameters on hydraulic zone through the methods regarding to hydraulic zone visualization.

We introduce a composite dimensionless parameter $Q_D = \log_{10}(Q/b^2KJ)$ according to Herrling et al. [18], the subscript D indicates that it is a dimensionless parameter. Q_D measures the ratio of flow rate of VCW and strength of ambient flow. The selection of this parameter is based on the knowledge that the flow pattern is dependent on the integrated effect of relevant factors. For example, keeping b and K constant, the flow pattern is then determined by Q/J, which means that if Q and J are simultaneously enlarged or reduced in the same proportion, the flow field will not change.

Another parameter we concern is the distance between the two screen centers d, dimensionless form is $d_D = d/b$. In this section, we assumed that the half-length for both injection and extraction screen is $L = 0.1b$, and the two screens are symmetrically installed with respect to the aquifer center. Thus, d_D value is constrained from 0.2 to 0.8.

5.1. Influence of VCW parameter on recirculation zone

In order to estimate the impact of Q_D and d_D on recirculation zone, we performed 90 simulations by combining nine values of Q_D and 10 values of d_D, and the geometric variables were recorded and analyzed. Notice that LR, WR and HR are the length, width and height for half of the recirculation zone, respectively. Contour plots in Fig. 5 are drawn by using their dimensionless form, $LR_D = LR/b$, $WR_D = WR/b$, $HR_D = HR/b$, b is the aquifer thickness. We define another parameter Recirculation Fraction RF, a ratio Q_R/Q, here Q is the total flow rate outflow from injection screen, and Q_R is a portion of Q, representing the amount of water recirculated.
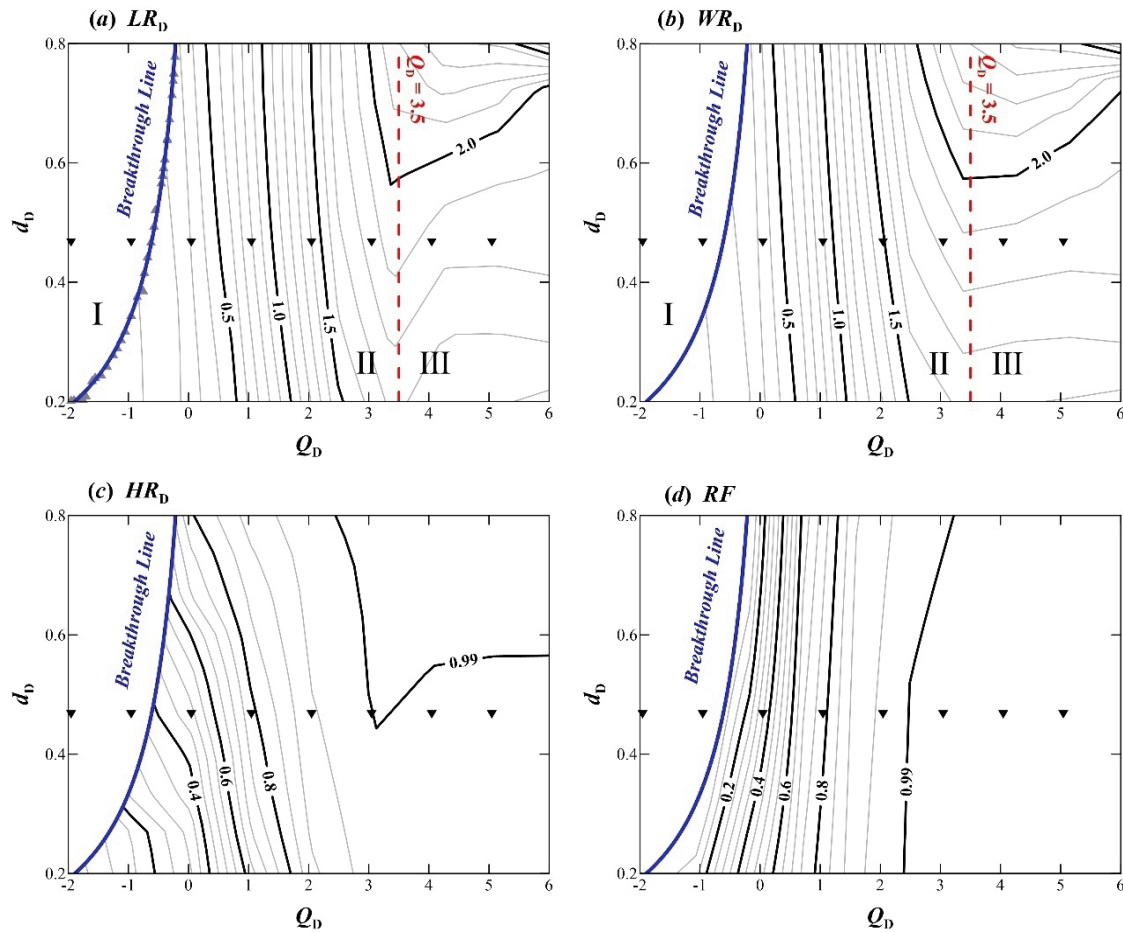
Fig. 5. Contour plots of geometric variable (a) LR_D, (b) WR_D, (c) HR_D of Re-circulation Zone and (d) RF for varying Q_D and d_D combinations. The dark inverted triangles scattered in each plot corresponding to the eight cases in Fig. 3.

Accordingly $Q-Q_R$ stands for the amount of water discharged from injection screen. Therefore, RF can also be referred to as a parameter to measure the efficiency of VCW circulation.

The plot (a) in Fig. 5 illustrates that the variation of LR_D with Q_D and d_D can be roughly divided into three parts. The first one is on the top left of the plot, where all $LR_D = 0$, meaning no circulation occurs due to either relative small Q_D or large d_D. It is apparent that circulation flow cannot be generated if the injection is too far away from the extraction screen. The Part One is separated with others by a Breakthrough Line, which was established by following two steps. First, we took 32 Q_D-d_D samples by applying a search procedure to find out the critical d_D values for each individual Q_D, as marked by the grey triangles in plot (a). Then, the breakthrough line can be determined by using fitting technique given sufficient samples. We finally found they were fitted well with a power function as Eq. (13), the R-square was as high as 0.9959.

$$Q_{D\_BT} = -0.4568 \times d_{D\_BT}^{-0.9901} + 0.3542 \tag{13}$$

The second part in plot (a) is between the breakthrough line and a vertical line approximately at $Q_D = 3.5$. LR_D is in direct proportion with both Q_D and d_D in this area, Q_D is

however, more influential. For the same Q_D, LR_D just slightly increases with d_D. The third part is for Q_D larger than 3.5, where the effect of d_D becomes dominant. LR_D is significantly increasing with a larger d_D, however a larger Q_D doesn't necessarily lead to a greater LR_D.

Plot (b) in Fig. 5 presents the variation of WR_D. It shows the similar pattern as LR_D. The three parts can be recognized as well. The variation of HR_D is displayed in plot (c), in which $HR_D = 1$ means the recirculation zone has reached both the top and bottom confining layer. As Q_D and/or d_D increases, the HR_D increases. A comprehensive analysis indicates that while Q_D larger than 3.5, the extent of recirculation zone is almost unaffected by value of Q_D, this is probably due to the effect of the confining boundaries.

Plot (d) in Fig. 5 shows the recirculation fraction RF as a function of Q_D and d_D. It illustrates that when Q_D is smaller than 3, the RF increases as Q_D increases and/or d_D decreases. Increasing Q_D or decreasing d_D increases the overall influence of the system on the ambient background flow. Hence, at the higher flow rates Q or decreased distances between screens d, it is easier for the system to circulate water, increasing the recirculation fraction of the system. When Q_D is larger than 3, RF will be greater than 0.99. This indicates that almost all water from injection screen eventually enter extraction screen, and all complete the circulation.
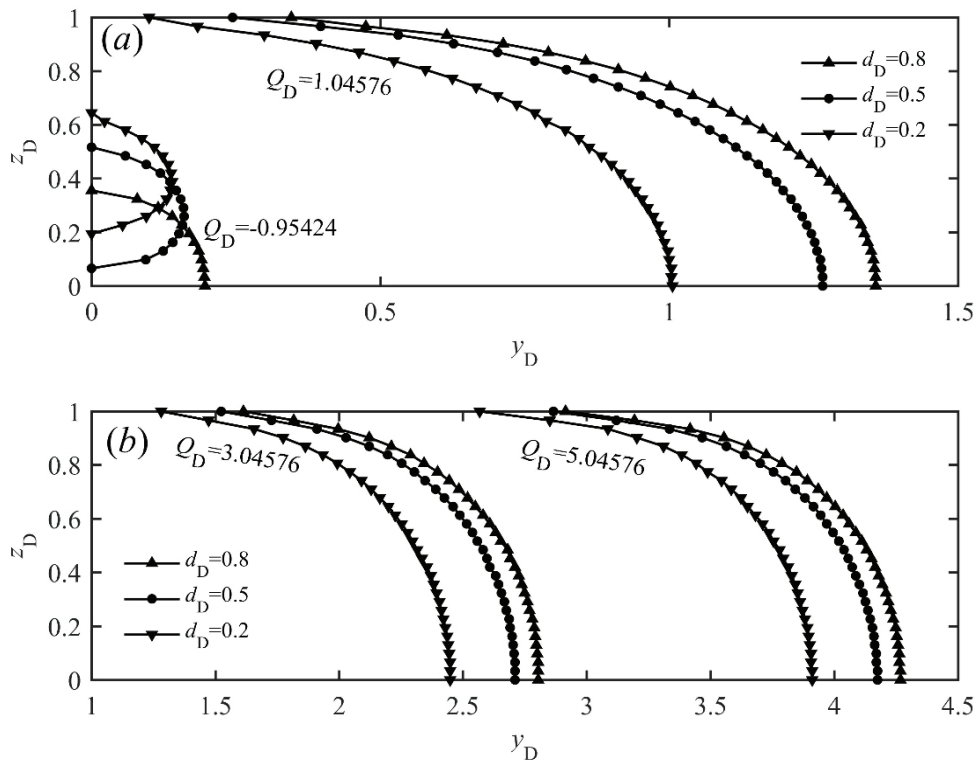
Fig. 6. Comparison for outline curves of capture zone for different Q_D and d_D combinations. Q_D is –0.95424 and 1.04576 in plot (a), and is 3.04576 and 5.04576 in plot (b). Dimensionless coordinates are $y_D = y/b$, $z_D = z/b$. Only a half of curve is presented due to its symmetry.

5.2. Influence of VCW parameter on capture zone

Twelve calculations were carried out for geometry analysis of capture zone by using 12 Q_D–d_D combinations. Fig. 6 presents the curves of half capture zone outline for different Q_D and d_D. These curves are obtained on a Y–Z cross section of a sufficient distance upstream from VCW, representing the ultimate width of the capture zone. It is not necessary to discuss the shape of discharge zone because of its symmetry with capture zone.

Generally, the capture zone size increases as Q_D increases. For the same Q_D, as d_D increases the width of capture zone increases as well. This is probably because increasing the separation distance reduces the short circuiting of flow between extraction and injection zones [19]. It is worth mentioning that when Q_D is larger than 3.5, increasing Q_D no longer enlarges the recirculation zone as noticed before, on the contrary, a larger Q_D certainly leads to a wider capture zone.

For small values of Q_D, the capture zone could not occupy the entire aquifer thick as shown in Fig. 6(a) for Q_D = –0.95424. This implies that for remediating a plume, a minimum Q_D might be required. When d_D decreases as the two screens get closer toward the center of aquifer, the capture zone will be moving upwards as a result.

6. Conclusion

In order to visualize 3D steady-state flow field induced by a vertical circulation well in a confined aquifer in presence of ambient flow, a mathematical model for spatial distribution of velocity is established based on superposition theory.

The fourth-order Runge-Kutta method is applied to perform particle tracking, and a critical value search procedure is developed to precisely construct 3D surface that delimits different hydraulic zones. The visualization illustrates that three hydraulic zones can be identified, namely the recirculation, capture, and discharge zones. The flow regime exhibits symmetry with respect to the central plane in the direction of ambient flow, and axis-symmetry regarding to the central line, given the injection and extraction screens are installed symmetrically.

The proposed visualization technique is also employed to investigate how the VCW parameters affect the geometry of hydraulic zones. Two dimensionless parameter Q_D and d_D are examined, where $Q_D = \log_{10} (Q/b^2 KJ)$ represents the integrated effect of VCW flow rate and strength of ambient flow, and $d_D = d/b$ measures the distance between injection and extraction screens. Simulation results demonstrate: (1) a Q_D–d_D breakthrough line can be established to mark the occurrence of circulation flow; (2) the size of recirculation zone is primarily determined by Q_D when less than 3.5, on the contrary it mainly depends on d_D while Q_D is larger than 3.5; (3) increasing Q_D and/or decreasing d_D results in more portion of circulation flow; (4) generally Q_D increases and/or d_D increases, the capture zone extend as well as the discharge zone.

As aforementioned, the vertical circulation well method has been widely used to remediate the contaminated aquifer. We have already achieved the visualization of hydraulic zones around a VCW in presence of ambient flow in this study, however, it will be more interesting and meaningful to investigate the extra solute transport under the similar conditions in spite of more complexities involved such as the

dispersion of solute and the chemical reaction between the reagent and contaminant. Thereby, future work can involve: (1) to investigate the solute transport with ambient flow; (2) to explore the temporal and spatial development of hydraulic or chemical zones; and (3) to determine the optimal placement between multiple VCWs given a contaminant plume.

Acknowledgement

References

[1]   V. Zlotnik, G. Ledder, Theory of dipole flow in uniform anisotropic aquifers, Water Resour. Res., 32 (1996) 1119–1128.
[2]   B.D. Alleman, Groundwater Circulating Well Assessment and Guidance, Battelle Memorial Institute, Columbus, USA, 1998.
[3]   W.E. Allmon, L.G. Everett, A.T. Lightner, B. Alleman, T.J. Boyd, Groundwater Circulating Well Technology Assessment, Citeseer, 1999.
[4]   M.N. Goltz, J.A. Christ, In: Delivery and Mixing in the Subsurface: Processes and Design Principles for In Situ Remediation, Springer, New York, 2012, pp. 139–168.
[5]   Y. Jin, E. Holzbecher, M. Sauter, Dual-screened vertical circulation wells for groundwater lowering in unconfined aquifers, Groundwater, 54 (2016) 15–22.
[6]   A.R. Kacimov, Y.V. Obnosov, A. Al-Maktoumi, Dipolic Flows relevant to aquifer storage and recovery: strack's sink solution revisited, Transport Porous Med., 123 (2018) 21–44.
[7]   R.C. Knox, D.A. Sabatini, J.H. Harwell, R.E. Brown, C.C. West, F. Blaha, C. Griffin, Surfactant remediation field demonstration using a vertical circulation well, Groundwater, 35 (1997) 948–953.
[8]   O.A. Cirpka, P.K. Kitanidis, Travel-time based model of bioremediation using circulation wells, Groundwater, 39 (2001) 422–432.
[9]   Y. Zhao, D. Qu, R. Zhou, S. Yang, H. Ren, Efficacy of forming biofilms by *Pseudomonas migulae* AN-1 toward in situ bioremediation of aniline-contaminated aquifer by groundwater circulation wells, Environ. Sci. Pollut. R., 23 (2016) 11568–11573.
[10] W. Burns, New single-well test for determining vertical permeability, J. Petrol. Technol., 21 (1969) 743–752.
[11] V. Zlotnik, B. Zurbuchen, T. Ptak, The steady-state dipole-flow test for characterization of hydraulic conductivity statistics in a highly permeable aquifer: Horkheimer Insel site, Germany, Groundwater, 39 (2001) 504–516.
[12] T. Halihan, V.A. Zlotnik, Asymmetric dipole-flow test in a fractured carbonate aquifer, Groundwater, 40 (2002) 491–499.
[13] V. Zlotnik, B. Zurbuchen, Dipole probe: design and field applications of a single-borehole device for measurements of vertical variations of hydraulic conductivity, Groundwater, 36 (1998) 884–893.
[14] S. Hvilshøj, K.H. Jensen, B. Madsen, Single-well dipole flow tests: parameter estimation and field testing, Groundwater, 38 (2000) 53–62.
[15] Z.J. Kabala, The dipole flow test: a new single-borehole test for aquifer characterization, Water Resour. Res., 29 (1993) 99–107.
[16] D.J. Sutton, Z.J. Kabala, D.E. Schaad, N.C. Ruud, The dipole-flow test with a tracer: a new single-borehole tracer test for aquifer characterization, J. Contam. Hydrol., 44 (2000) 71–101.
[17] J.S. Chen, C.W. Liu, Y.C. Chan, C.F. Ni, K.K. Kao, Effect of transverse dispersion on solute transport in a vertical dipole flow test with a tracer, J. Hydrol., 402 (2011) 206–216.
[18] B. Herrling, J. Stamm, W. Buermann, In: In Situ Bioreclamation, Butterworth-Heinemann, 1991, pp. 173–195.
[19] R.D. Philip, G.R. Walter, Prediction of flow and hydraulic head fields for vertical circulation wells, Groundwater, 30 (1992) 765–773.
[20] J. Huang, M.N. Goltz, A three-dimensional analytical model to simulate groundwater flow during operation of recirculating wells, J. Hydrol., 314 (2005) 67–77.
[21] R.L. Johnson, M.A. Simon, Evaluation of groundwater flow patterns around a dual-screened groundwater circulation well, J. Contam. Hydrol., 93 (2007) 188–202.
[22] J.S. Chen, C.S. Jang, C.T. Cheng, C.W. Liu, Conservative solute approximation to the transport of a remedial reagent in a vertical circulation flow field, J. Hydrol., 390 (2010) 155–168.
[23] O.D.L. Strack, Groundwater Mechanics, Prentice Hall, Englewood Cliffs, 1989.
[24] B.A. Faybishenko, I. Javandel, P.A. Witherspoon, Hydrodynamics of the capture zone of a partially penetrating well in a confined aquifer, Water Resour. Res., 31 (1995) 859–866.
[25] D.C. Schafer, Determining 3D capture zones in homogeneous, anisotropic aquifers, Groundwater, 34 (1996) 628–639.
[26] C. Muffels, X. Wang, A. Matthew Tonkin, C. Neville, User's Guide for mod-PATH3DU: A Groundwater Path and Travel-Time Simulator, SS Papadopulos & Associates, Inc, 2014.